INFRARED DETECTION OF CONCRETE DETERIORATION

by

R. H. Arnold

H. L. Furr

J. W. Rouse, Jr.

TECHNICAL REPORT RSC-02

July 1969

Supported in Part by

National Aeronautics and Space Administration

NASA Grant ~~NsG-239-62~~

NGL-44-001-001

TEXAS A&M UNIVERSITY

REMOTE SENSING CENTER

COLLEGE STATION, TEXAS

INFRARED DETECTION OF CONCRETE DETERIORATION

by

R.H. Arnold, H.L. Furr, and J.W. Rouse, Jr.

I. INTRODUCTION

Concrete deterioration on roadways and bridges poses a major problem to highway safety and maintenance. Means of detecting the rate and type of deterioration have been under investigation with increasing emphasis in recent years. Acoustic techniques have shown promise in this area, but a method of performing the evaluation rapidly over large areas is needed.

The recent emphasis on remote sensing technology research especially in connection with the NASA Earth Resources Program, has encouraged experimentation with sensors over a wide range of the frequency spectrum. This report summarizes results of a preliminary experiment to ascertain the feasibility of determining concrete deterioration by measuring thermal emissivity in the 2 to 5 micron region of the infrared spectrum. The experiment has a very limited scope due to its fundamental exploratory nature. This effort constitutes an initial phase of an ongoing research program conducted by the Texas Transportation Institute and the Remote Sensing Center, Texas A & M University.

II. BASIS

The experiment is based on the premise that the surface emissivity of a concrete structure is a function of its internal homogeneity. Emissivity is proportional to the rate of heat energy exchange at the surface-air interface. This energy flow is a function of the sub-surface character of the structure.

Faults, such as delaminations, alter the normal heat flow within the structure and conceivably will affect the surface emissivity in the region of the fault. Surface scaling and vertical cracking influence surface emissivity but these are surface effects and are easily detected by eye. Delamination, on the other hand, is generally hidden and is more difficult to detect.

It is believed that during heat transfer to the structure, delaminated areas will rise in temperature more rapidly than the homogeneous areas surrounding the fault. During heat transfer from the structure, the delaminated region should cool more rapidly. Since both faulty and solid regions have equal initial and final steady-state temperatures, the detection of the existence of a delaminated area, if possible, is closely related to some unknown time period within the interval during which heat exchange occurs. Determining the feasibility of infrared detection of concrete delaminations was the fundamental basis of this preliminary work.

III. CONCRETE DETERIORATION

Concrete is generally a very durable construction material, and it serves well under severe service through a wide range of atmospheric conditions. It is destructable, however, and conditions of construction, service, and atmospheric extremes sometimes combine to cause its deterioration. Exposed concrete such as that in highway and airport pavements and bridge decks accounts for the major portion of the deterioration. This investigation is directed toward detecting deterioration in concrete used in such structures.

A major deterioration type is surface scaling and it is caused by a gradual erosion of surface material. Generally such a condition is brought about by freeze-thaw action, the use of de-icing chemicals during freezing weather, and improperly designed concrete mixes. This type of deterioration is easily detected by eye without the aid of elaborate aids, and it is not treated further here.

Vertical cracking begins at the surface and works inward. The depth of such cracks varies from very shallow to completely through the depth of the slab. They are caused by shrinkage during curing of the concrete, contraction due to thermal changes, stresses from service loads, or combinations of these. Most of these cracks are very narrow. Vertical cracks provide access for contaminants to enter the interior of the concrete. They are usually visible to the eye and generally require no detection equipment.

Interior cracking along planes more or less parallel to the surface of the structure delamination, are usually not visible, and detection is sometimes difficult. It is this type of deterioration which is of primary interest in this investigation.

IV. TEST SPECIMENS

Seven portland cement concrete specimens were used in the experiment. They were set up in an unshaded area, and the experiments were made in June during warm weather. The samples exhibited both vertical and horizontal fractures or simulated fractures in accordance with the objectives of the experiment. Samples featuring controlled horizontal striations at varying depths were included in the data sample. They are described in detail below.

Specimen I, (Fig. 1a), is a 7 inch thick structural lightweight concrete slab approximately 3 feet square and is elevated 2 feet 9 inches above the ground. The slab is in sound condition and has a smooth surface texture. The top surface is divided into 4 square areas approximately 18 inches on a side, three areas having concrete overlays and the fourth area, area A, in the original condition. Area B has a 1 5/8 inch thick, rough surface, bonded overlay. Area C has a 1 5/8 inch thick, rough surface, unbonded overlay, and Area D has a 3/4 inch thick, rough surface, unbonded overlay. A layer of polyethylene plastic separates the C and D overlays from the slab. The overlays are separated by one inch spacings, are subject to ambient air temperature at all edges, and are of normal weight concrete.

Specimen II, (Fig. 2a), is a three foot square area of a 10 foot wide octagonal slab, 7 inches thick. It is lightweight concrete, 4 years old, and was tested to failure in another program. This octagonal slab has cracks, almost parallel to the plane of the slab, at varying depths at the center and extending to about two feet from the center. The slab was elevated above the ground approximately 28 inches and contains 5/8 inch diameter steel reinforcing bars, approximately 6 inches apart and 3/4 inch below the surface. Specimen II is an outer portion of the slab, consisting of both sound and fractured portions. The surface was the bottom of the slab when cast and has a smooth texture over the sound portion.

Specimen II, (Fig. 3a), is another section of the lightweight slab containing Specimen II. This specimen is a three foot square area with overlays designed and arranged as Specimen I. The overlays are of the same type of concrete as the slab. This section was chosen such that areas A, B, C, and D have equal parts of sound and delaminated under-structure. The slab surface has a smooth texture with only slight occasional cracks. The overlays, as in Specimen I, have a rough surface texture and are separated by one inch spacings.

Specimen IV, (Fig. 4a), is a three foot square area of a concrete pavement. This 25 year old pavement of normal weight concrete has a rough surface texture. The entire pavement surface is sound. The specimen has four areas with the three types of overlays of the same design and type as Specimen I.

Specimen V (Fig. 5a), is another section of the octagonal slab. It contains several exposed reinforcing bars due to concrete separation and removal. The dark area in the center of the photo shows exposed aggregate and slopes from the surface to the bars; this exemplifies spalling. The surface area surrounding the niche (spalled area) contains solid and subsurface delaminated portions.

Specimen VI, (Fig. 6a), is a round lightweight slab of the same type as the octagonal slab. It contains areas of sound and delaminated concrete and is used only as an additional specimen for support data.

Specimen VII, (Fig. 7a), is a square, lightweight slab of the same type as the octagonal slab. The center is delaminated and the edges are solid. The exposed aggregate is sound. The ends of four vertical bars at the center of the slab appear as a square array of dots, figure 7b. This specimen is used for additional support data.

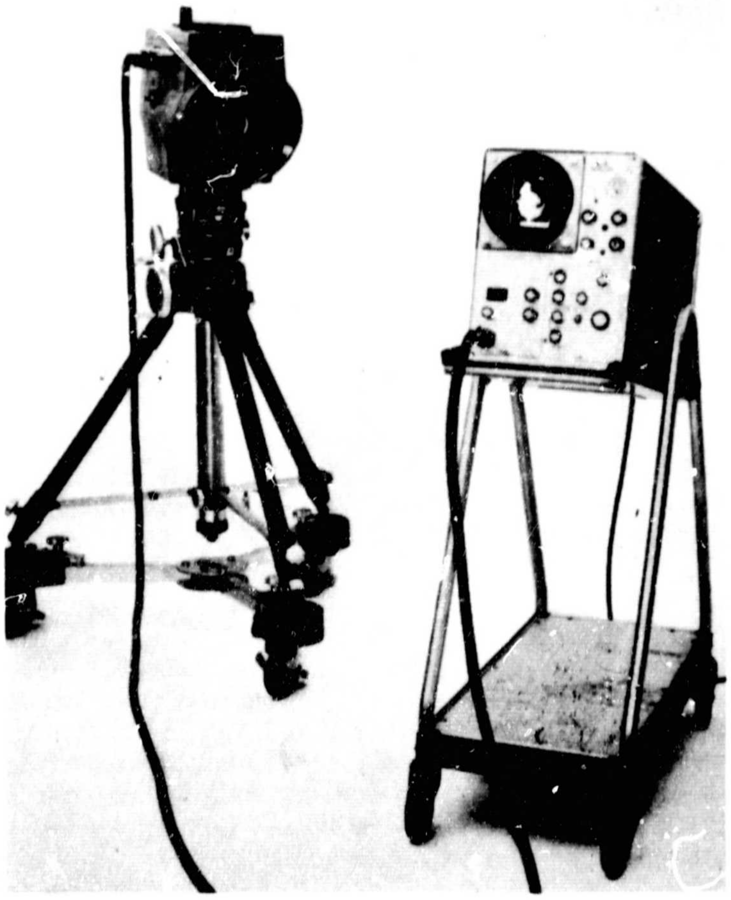

Figure 1. AGA Thermovision is built up of two basic units camera unit and display unit.

Figure 2. The basic parts in the camera unit are the spherical mirror, the oscillating plane mirror, the rotating silicon prism and the InSb IR-detector.

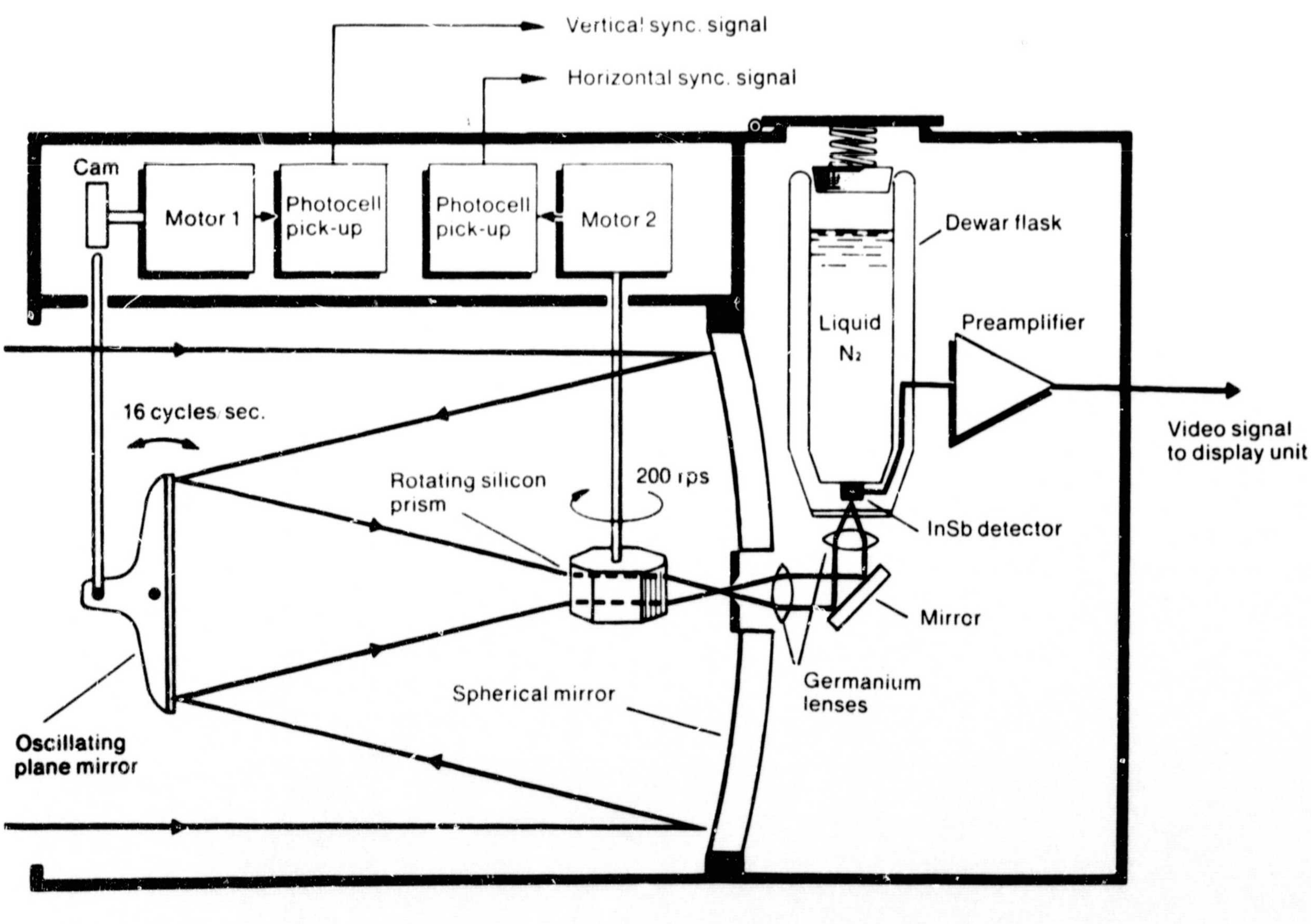

V. SET UP FOR RECORDING DATA

With the samples arranged in close proximity, a lift truck was used to elevate the recording equipment 17 feet above the ground. The viewing angle for specimens I and IV was 40° from the nadir, and for specimen II and III, 38°; for specimen V, 33°, and for specimen VI, 25°.

The field of view of the scanner is limited to 5° by 5°. Therefore, only about one-half the area of specimens I through V were visible at each position. All but the outlying portions of specimen VII was visible. Various specimen portions were scanned to completely observe the infrared differences.

VI. INFRARED CAMERA

The infrared scanner employed in this experiment was developed and manufactured by the Swedish Company AGA AB. The infrared detector used in the AGA Thermovision is an indium antimonide detector (InSb), with the typical time constant of one microsecond. The picture frequency of this instrument is 16 frames per second. The equipment consists of a camera unit and a display unit. The infrared radiation from the object is collected by a spherical mirror that focuses the radiation via a secondary mirror onto the detector. The horizontal scanning is performed by an 8-sided silicon prism rotating at 200 revolutions per second. The scanning function of the prism yields 1600 lines per second or 100 lines per frame. Vertical scanning is performed by means of a linear tilting motion of a secondary mirror. Mirror oscillation frequency is 16 Hz corresponding to the image rate of 16 frames per second. The temperature resolution of the system is approximately 0.2°C at room temperature and the spacial resolution is approximately 100 elements per line. The camera field of view is 5° by 5° and the focusing range is between 2.4 meters and infinity.

The video signal from the infrared detector is used to intensity modulate a raster on a cathode-ray tube. This display is termed a thermograph. Relative temperature differences appear as gray tone variations on a thermograph. Provisions are available for preselecting the range of temperatures to be displayed on the CRT. Such displays consititute isotherm pictures.

VII. DATA RECORDING

In order to determine optimal conditions for thermal detection of solid and delaminated concrete, infrared studies were made under a variety of conditions including various times of day.

Preliminary data for the specimens was taken on June 4, 1969 from 2:00 to 4:00 p.m. The previous three days had been rainy or overcast and damp. The fourth of June was heavily overcast with occasional sunshine on the specimen.

Various isotherms and thermograms of each specimen were made to determine which provided the most useful information. Thermograms provided more meaningful data. A schedule of morning and evening examinations of the concrete was devised to study the periods of heat transfer.

The initial experiment was performed during a 2 hour and 20 minute period beginning at 7:45 p.m. on June 5. The day had been hot, dry, and clear. A surface temperature thermometer was used to obtain air and concrete temperatures. Contact thermisters and thermometers were preferable, but were unavailable at the time of the tests. Twenty-five infrared photographs of specimens I through V were made. Equipment adjustment for darkness level, relative temperature level, and intensity were made to acquire good images.

At 5:45 a.m. on June 6 the second stage of the experiment began. Infrared photographs of various sections were made of each specimen. Morning sunlight reached specimen III at 7 a.m., specimen VI at 7:10 a.m., specimen I at 7:22 a.m., and specimen II at 7:26 a.m. As the sunlight on each specimen increased, differentiation between areas became more difficult due to radiation scatter from the specimens. Forty-five photographs were taken; eleven after 8:00 a.m. This phase ended at 9:30 a.m.

The final stage of the experiment began at 8:00 p.m., the evening of June 6. The day had again been hot and clear.

Photographs of selected specimens were taken under induced conditons. Water was applied to the surface of the specimens in a mopping action for about ten seconds. The excess water was brushed away. After two minutes another infrared photograph of the specimen was taken. Very good results were obtained from specimen II. Several other photographs were made of other areas. The experiment ended at 10:00 p.m.

VIII. DATA RESULTS

Plate I - Plates 1a and 1b contain tests results of specimen I. Photos 1b, 1c, and 1d are morning shots depicting area C as the coolest and A as the warmest, with B and D equivalent in 1b and slightly different at 1d. Relative temperature levels (RTL) are equal to ten degrees while the darkness levels (DL) vary. Photo 1e is the same thermogram (TG) as 1f except for an isotherm (IT) superimposed upon it. The concrete temperature is 80°F with the air temperature 75°F. Area B is about four degrees (4°F) warmer than area D. This difference began to appear 1 1/2 hours after sunset. The unbonded area (D) had cooled throughout. The bonded area (B) had cooled only on the edges. Photos 1g, 1h, and 1i show temperature differences between B and D at various periods. Figure 1g and 1h are an evening photograph of equal RTL and DL showing that area D became cool faster than B. Photo 1i, taken prior to sunrise, still shows area B warmer than D. Photo 1j, (areas A and C) shows area A (white) as being warmer two hours after sundown. Photos 1k and 1l show the TG and IT of the specimen. Taken on a cloudy afternoon, both 1k and 1l show area C as the warmest. The warm, light portion between the areas is wood at a higher temperature than most of the concrete.

Plate II - Plate II has test results of specimen II. Several metal rods were used to outline sections, as seen in the photos. Photos 2b and 2c, taken on a cloudy afternoon, show a rod lying on unsound areas having cracked underportions. The solid areas are very dark, while the delaminated areas are very white. In photo 2b deep cracks appear as light gray. Both photos have equivalent DL's and RTL's.

Photo 2d, taken in the evening, depicts a revision of shades. The rod was used to separate sound and unsound portions of concrete. At this time, the concrete was giving off heat, leaving the delaminated areas up to seven degrees cooler than the solid (RTL=10, DL's of 2 and 9 respectively). The solid areas are white and the delaminated areas gray to dark. Straight white lines running diagonally across the photos 2d, 2e, and 2f are the steel support bars under the surface.

Photos 2e, and 2f, evening shots, show delaminated areas as dark. The area shown in 2e was doused with 77°F water and allowed to dry for two minutes, after which photo 2f was taken. The focus is different for these two shots causing a darker appearance of the delaminated areas for 2f. Again the reinforcing bars can be seen.

Plate III- Plate III has test results of specimen III. Photo 3b, taken in the evening, shows area A as delaminated. Area C is the coolest area, and area B the warmest. Photo 3c, taken later in the evening, shows area D as having cooled faster than area B; D being relatively darker. The DL and RTL, changed between photos, affected the relative darkness of areas. Pictures 3d, 3e, and 3f area time sequence of morning shots. Photo 3d taken before sunrise shows the areas from warmest to coolest as A, B, D, C. As the sun was rising in 3e, the areas became indistinguishable. In 3f, the sun's reflection hampered differentiation of the small temperature differences of the concrete areas. The latter three photos have equal RTL's and similar DL's.

Plate IV- Plate IV contains test results of specimen IV. Pictures 4b, 4c, and 4d, taken in the evening, show area C as the coolest with a section of A cooler than B and D. Very little differentiation exists between B and D. Various RTL's and DL's were used to examine the specimen. Pictures 4e and 4f, taken in the morning, again show area C as the coolest. Photo 4f has poor resolution due to sunrays scattering off the surface. Equal RTL's and DL's were used.

Plate V - Plate V contains test results of specimen V. Picture 5b, evening shot, shows the solid concrete (upper-left) as warmer. A metal rod is in the solid section. The support rods are very warm while the delaminated concrete (lower-right) is coolest. The exposed aggregate is slightly cooler than the solid portion, Figures 5c, 5d, 5e, and 5f are a morning sequence. These show the same delineation as in 5b with resolution becoming worse as the sun's rays scatter more from the surface.

Plate VI - Plate VI contains test results of specimens VI and VII. Figure 6b shows delaminated areas at the cracks as cooler than the center or outlaying portions of the slab. Figure 6c shows the same area two minutes after water was doused on the specimen. A crack now appears at the center surface. With both picutres at equal RTL's and DL's, the doused slab is seen to be the cooler.

Figure 7b and 7c show a nighttime view (10:00 p.m.) of specimen VII. The delaminated inner portions appear cool, while the solid outer portions of the slab is warm. The four iron bars arranged in a square fashion at the center with their ends at the surface appear to be warmer than the surrounding delaminated concrete. The exposed, solid aggregate in the lower right hand portion of the pictures appears to be the warmest area.

IX. CONCLUSIONS

This experiment constituted a preliminary feasibility study of the use of thermal nondestructive detection of deteriorated concrete. The test results showed the existence of thermal emissivity differences related to certain deterioration conditions. Delaminations were detectable using an infrared scanner. They were most noticable during ambient cooling periods during heat transfer from the specimens. The experimental data justifies continued study and indicates the need for supporting information such as surface temperatures and radiometric measurements during the entire heat exchange intervals.

PLATE Ia

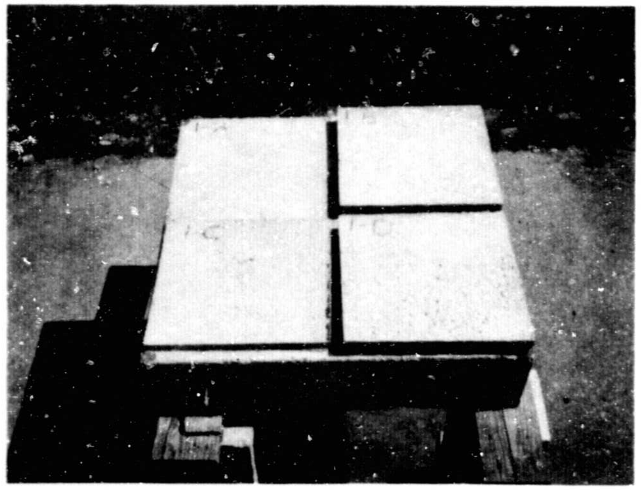

SPECIMEN I - 1a

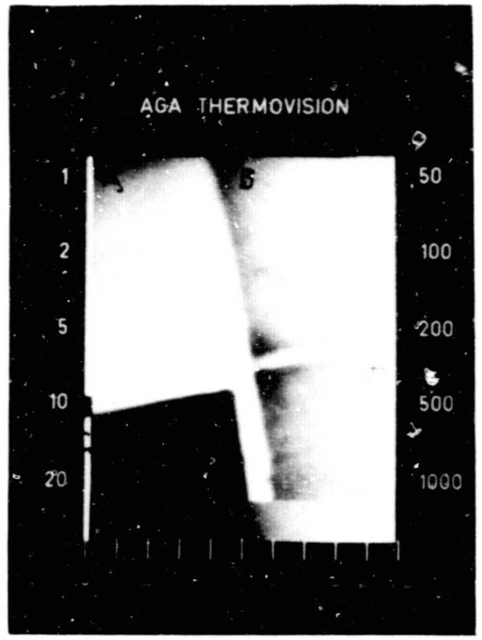

1b 6-5-69 8:00 p.m.
ABCD

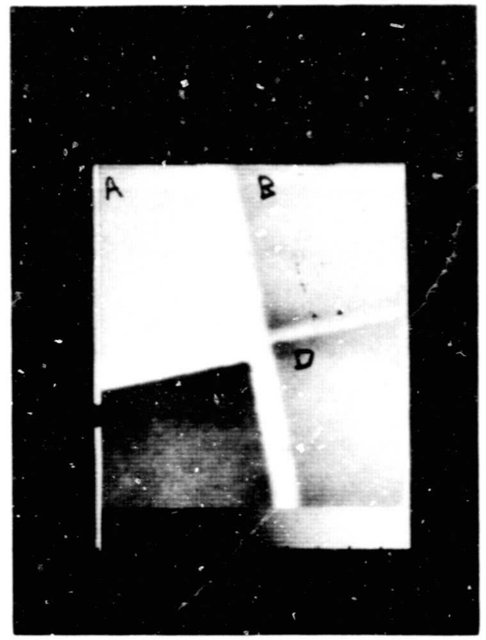

1c 6-5-69 8:20 p.m.
ABCD

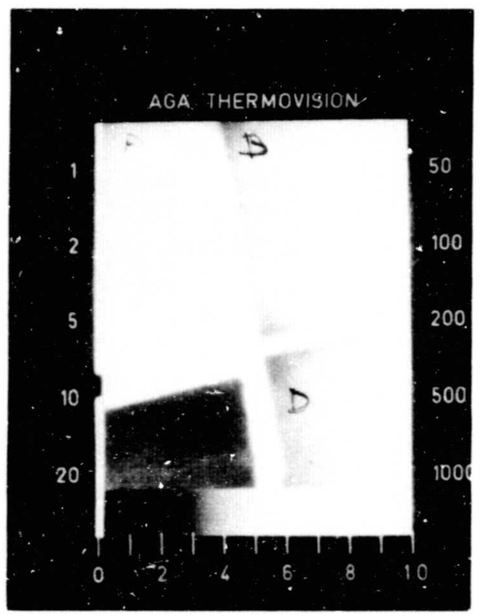

1D 6-5-69 8:40 p.m.
ABCD

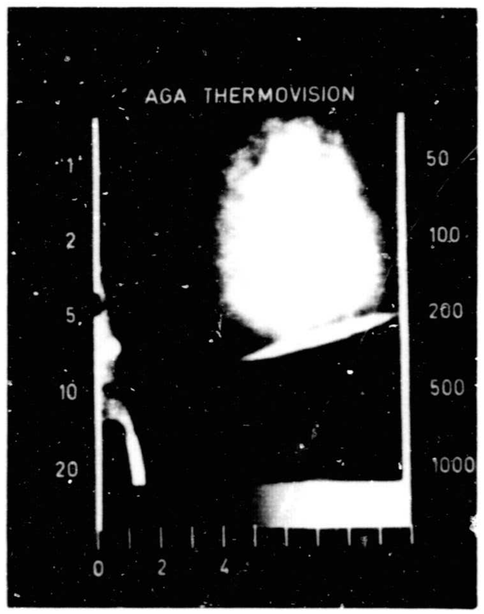

1e 6-5-69 9:10 p.m.
BD Isotherm

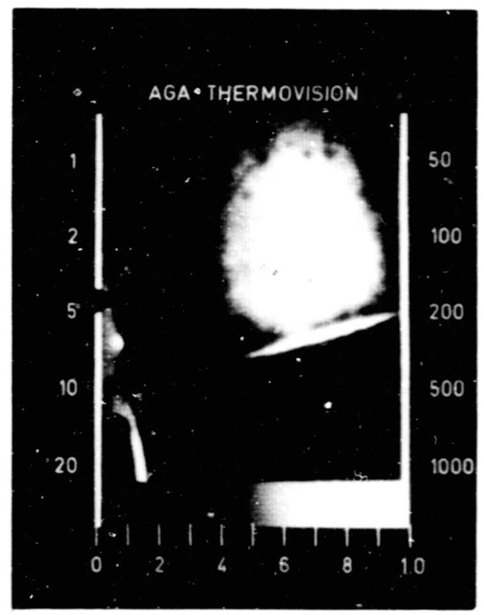

1f 6-5-69 9:10 p.m.
BD

PLATE Ib

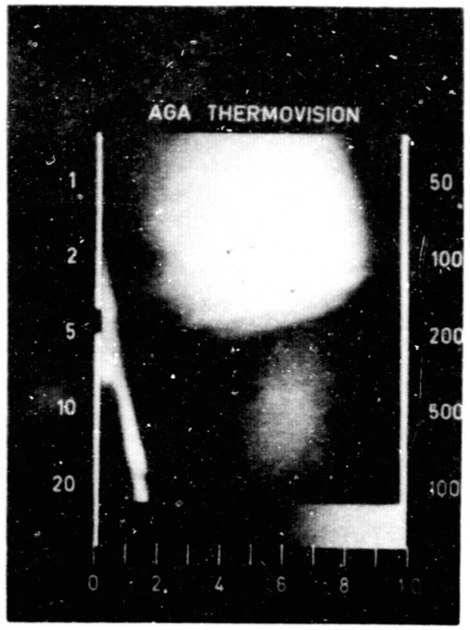

1g BD 6-5-69 9:23 p.m.

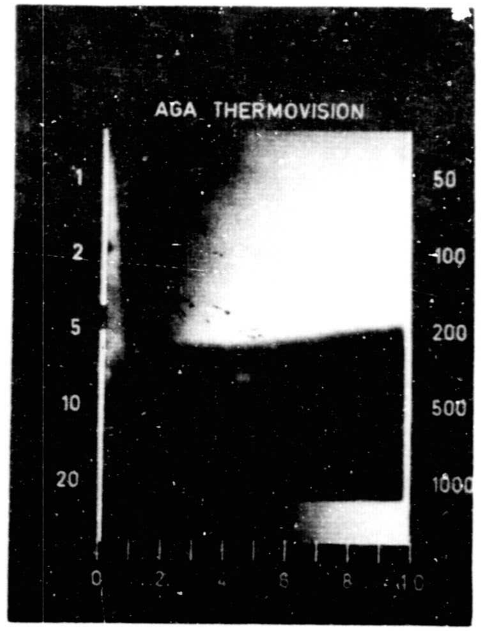

1h BD 6-5-69 9:23 p.m.

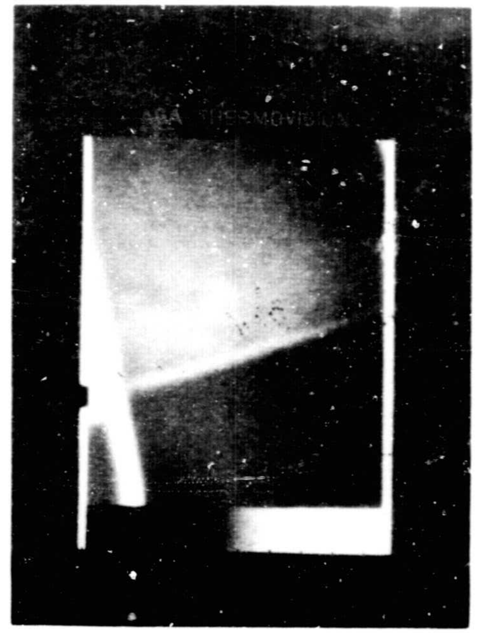

1i BD 6-6-69 5:45 a.m.

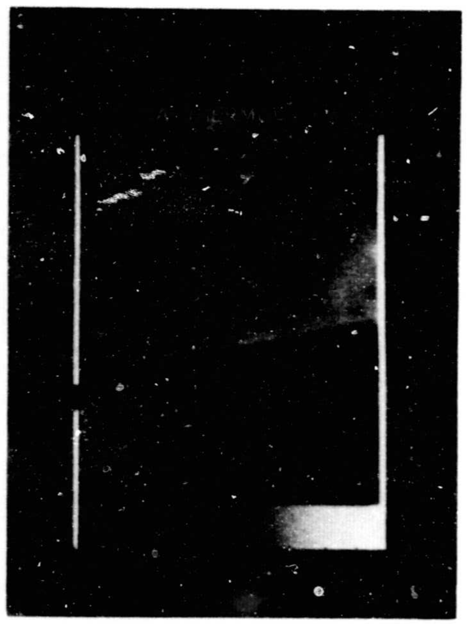

1j AC 6-5-69 10:05 p.m.

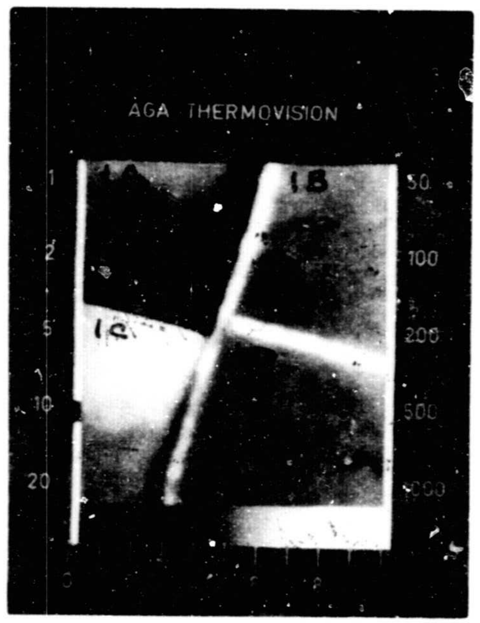

1k ABCD 6-4-69 Mid-Afternoon Cloudy

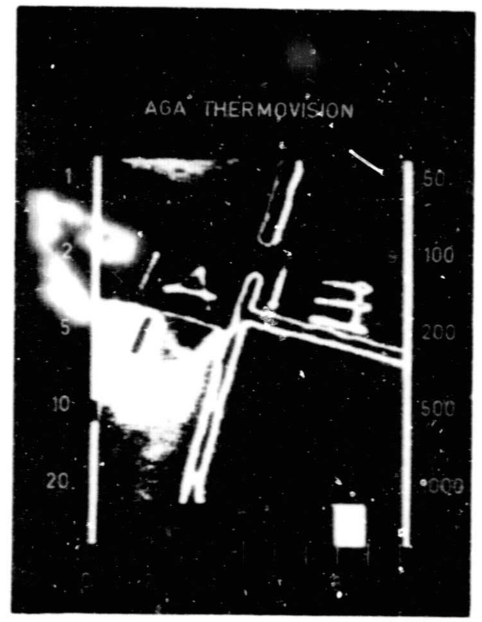

1l ABCD 6-4-69 Isotherm Mid-Afternoon Cloudy

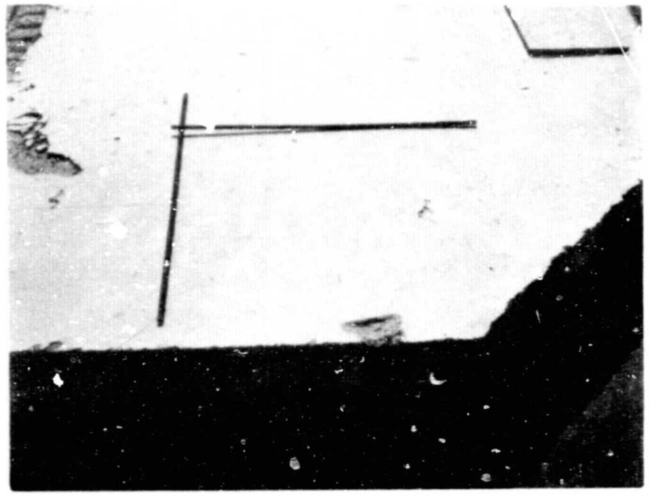

SPECIMEN II - 2a

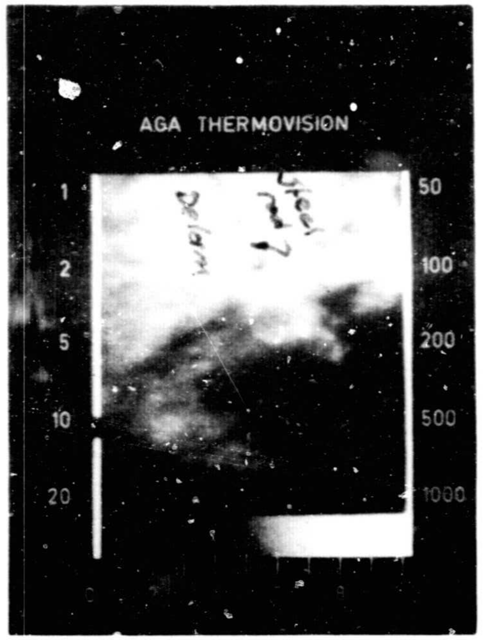

2b 6-4-69 Mid-Afternoon
solid (dark) vs. delaminated area

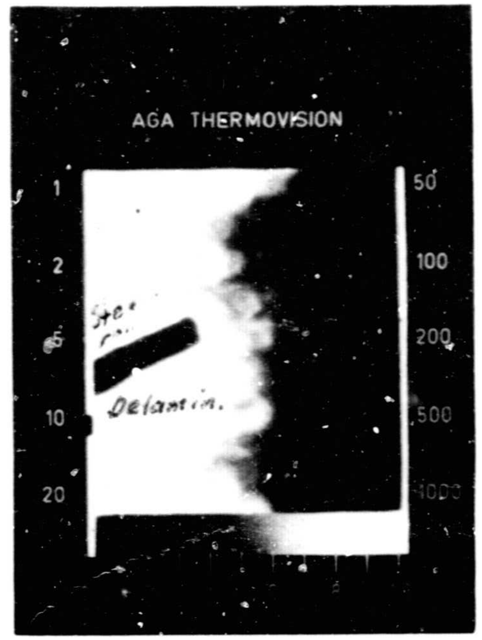

2c 6-4-69 mid-afternoon
rod in delaminated area cloudy

2d 6-5-69 8:08 p.m.
reinforcing rods showing through
solid & cracked area

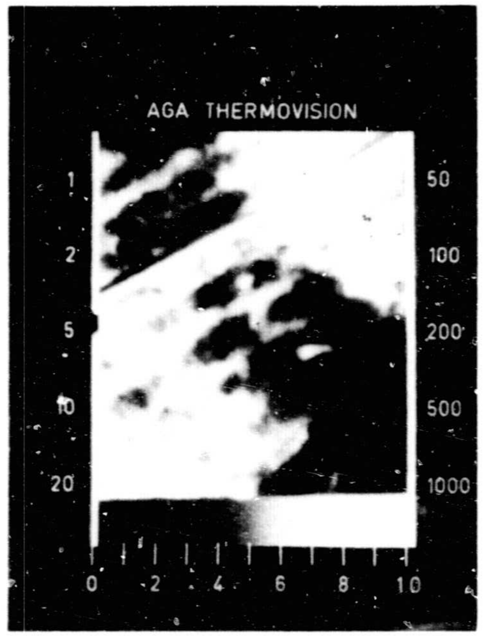

2e 6-6-69 8:05 p.m.
just shaded

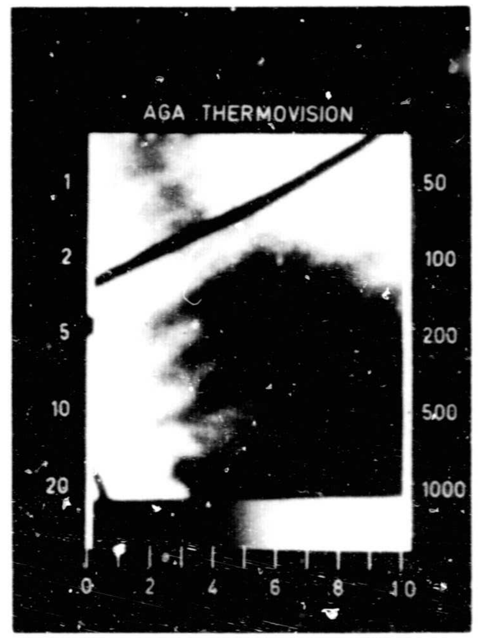

2f 6-6-69 8:08 p.m.
2min. after wetting with 77^{0}F water

PLATE III

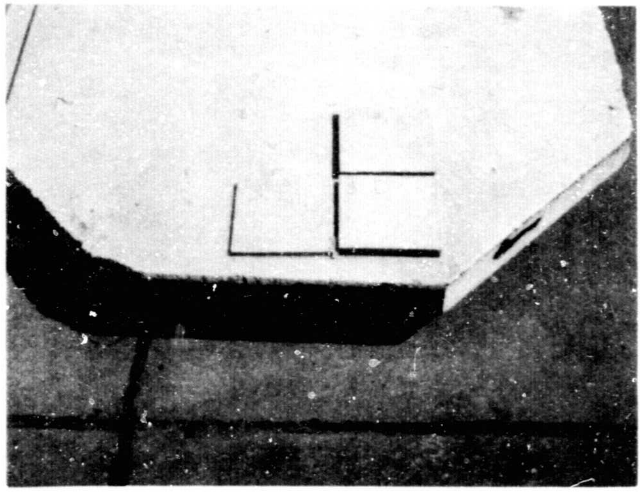

SPECIMEN III - 3a

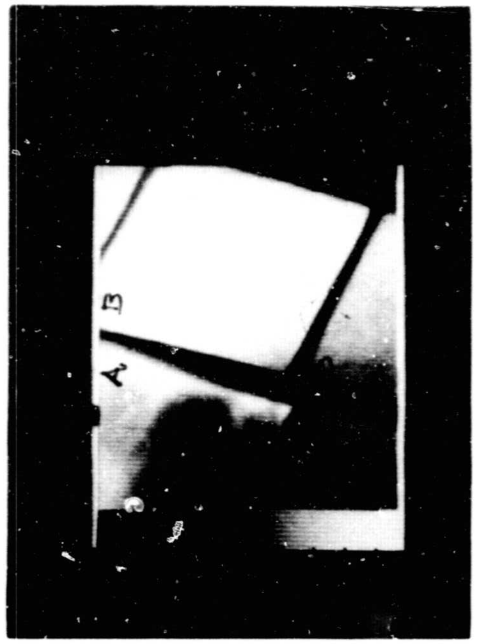

3b ABCD 6-5-69 8:25 p.m.

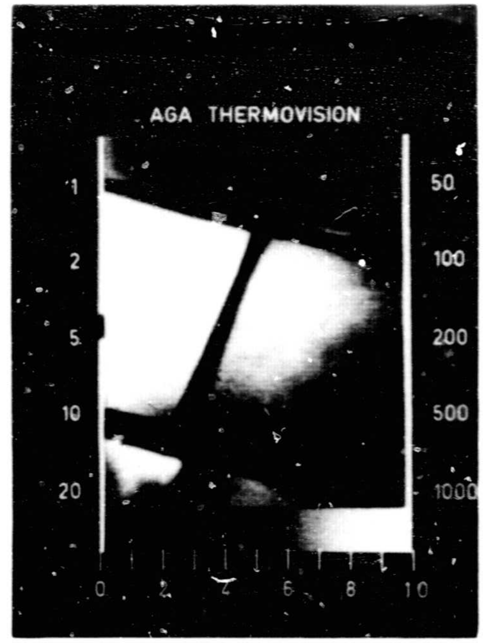

3c ABCD 6-5-69 9:30 p.m.

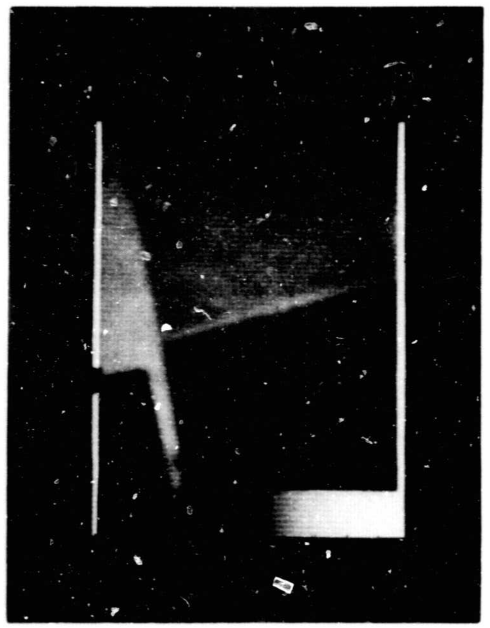

3d ABCD 6-6-69 6:15 a.m.

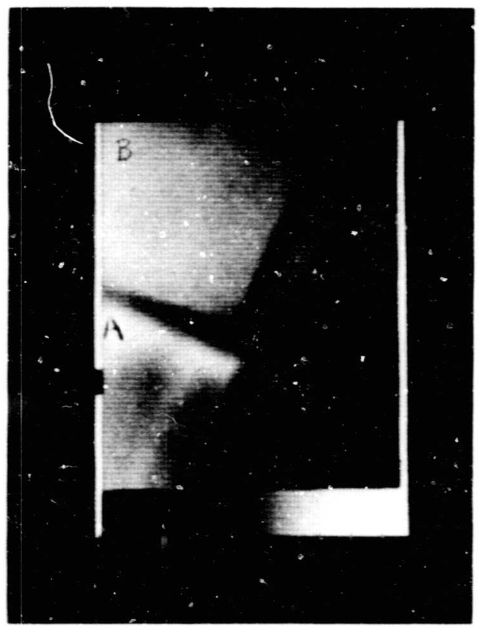

3e ABCD 6-6-69 7:00 a.m.
Just as sun hit corner

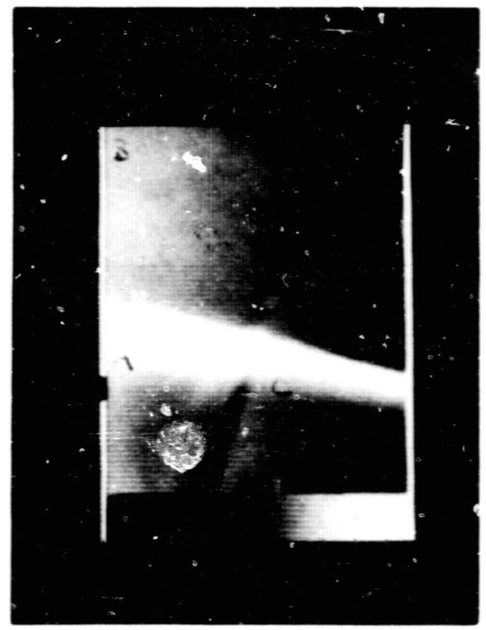

3f ABCD 6-6-69 7:39 a.m.

PLATE IV

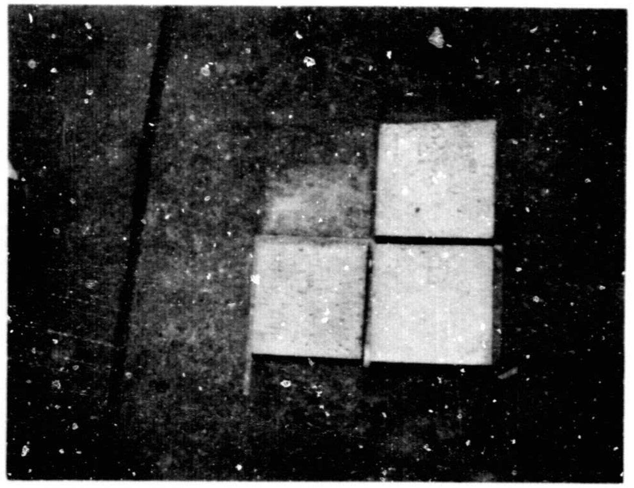

SPECIMEN IV - 4a

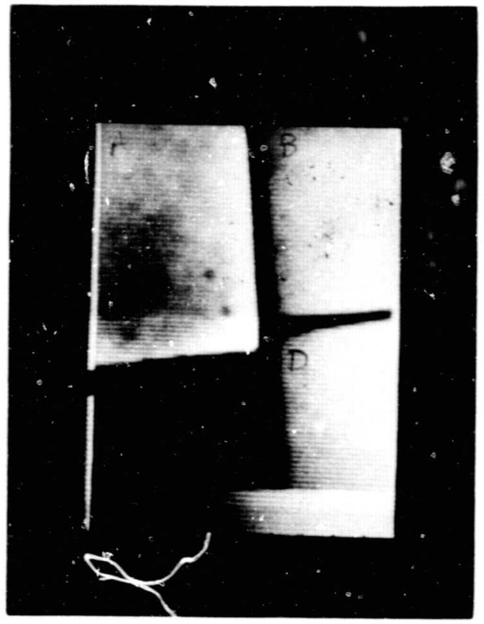

4b 6-5-69 8:34 p.m.
ABCD

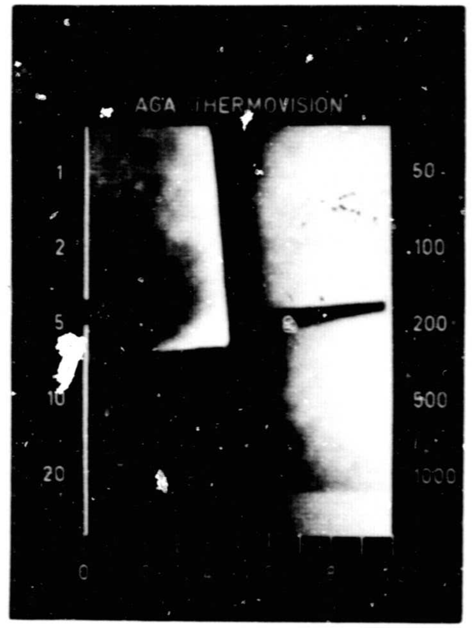

4c 6-5-69 9:15 p.m.

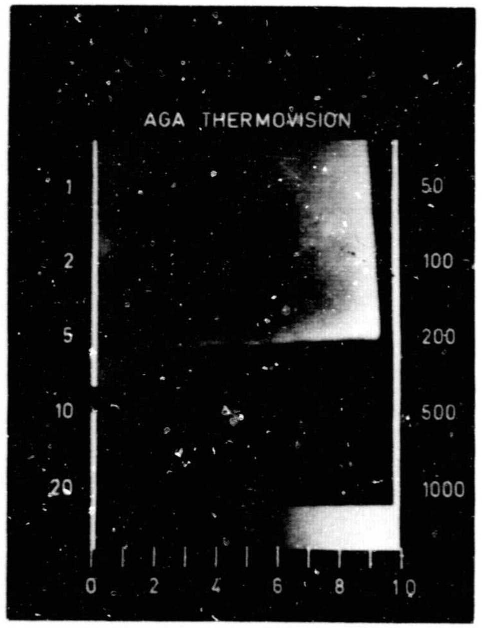

4d 6-5-69 9:40 p.m.
AC can't tell any difference between B & D now

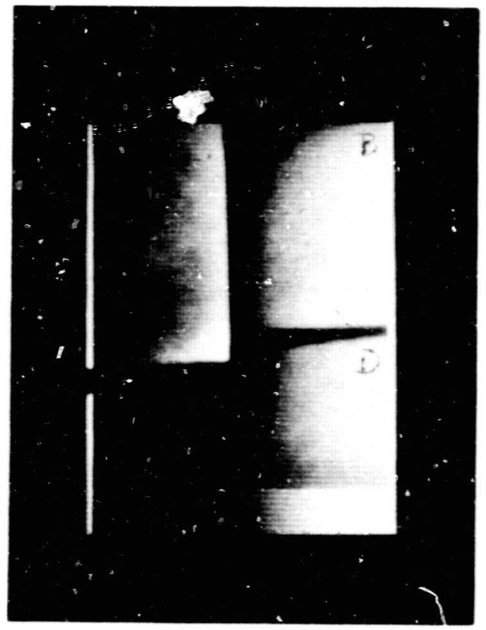

4e 6-6-69 7:00 a.m.
ABCD Shaded

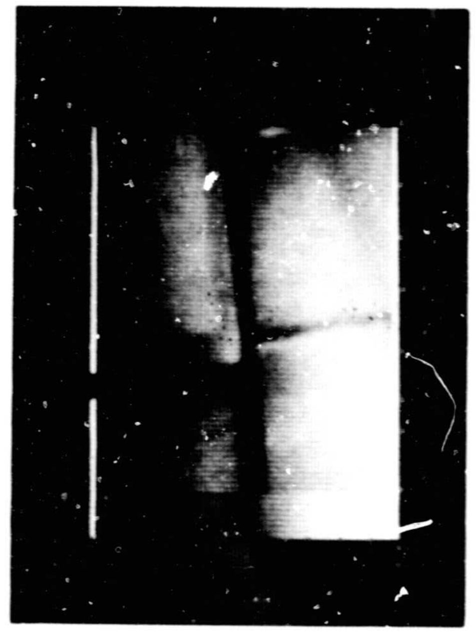

4f 6-6-69 7:43 p.m.
ABCD In Sun

PLATE V

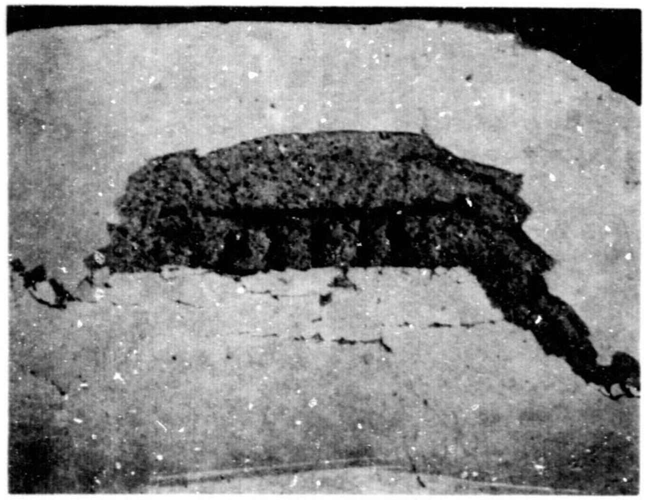

SPECIMEN V - 5a

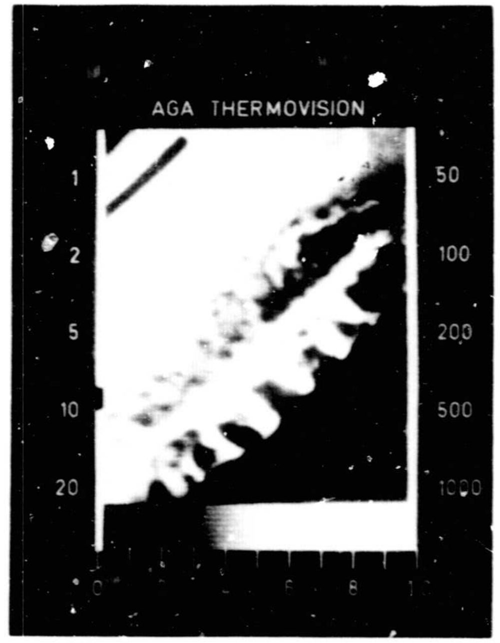

5b 6-5-69 8:40 p.m.
Isotherm

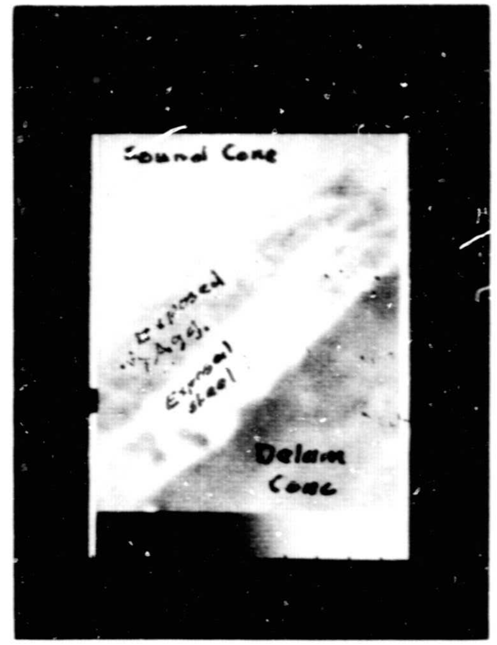

5c 6-6-69 6:06 a.m.

5d 6-6-69 6:55 a.m.

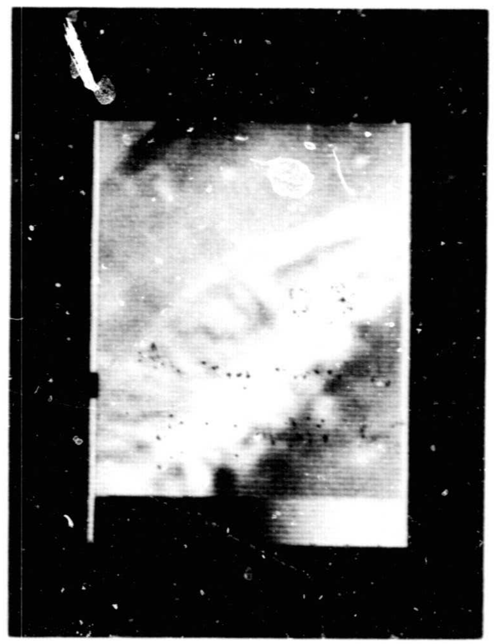

5e 6-6-69 7:28 a.m.

5f 6-6-69 8:35 a.m.

PLATE VI

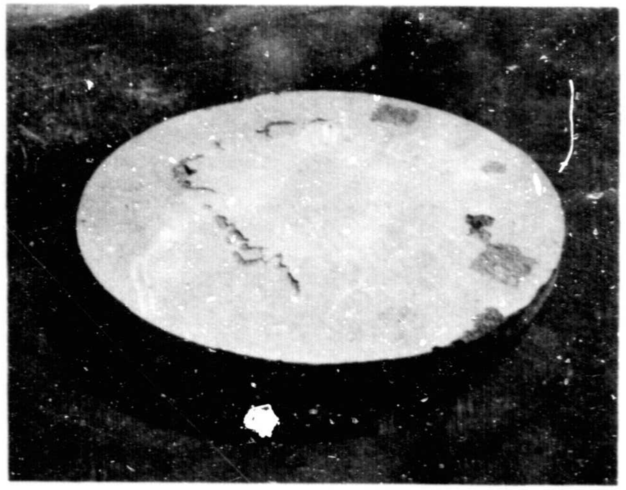

SPECIMEN VI - 6a

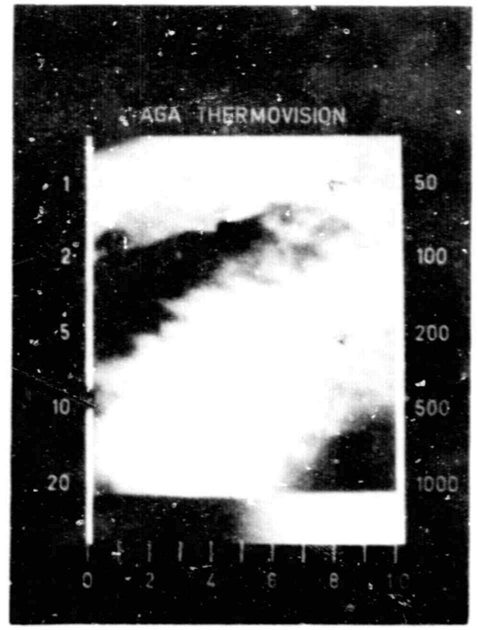

6b 6-6-69 8:25 p.m.
Dry

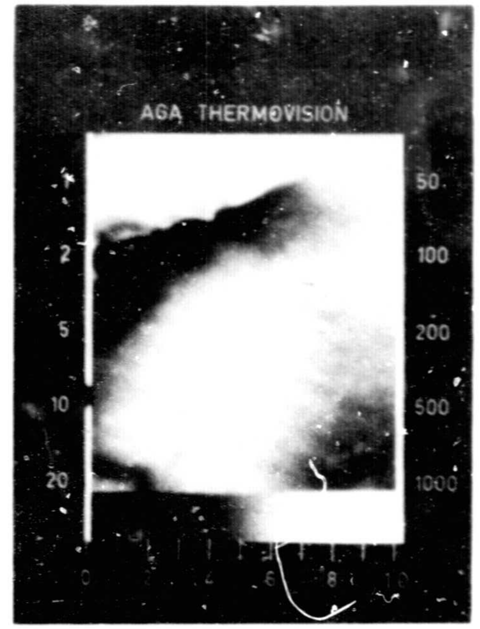

6c 6-6-69 8:30 p.m.
After flushing with water

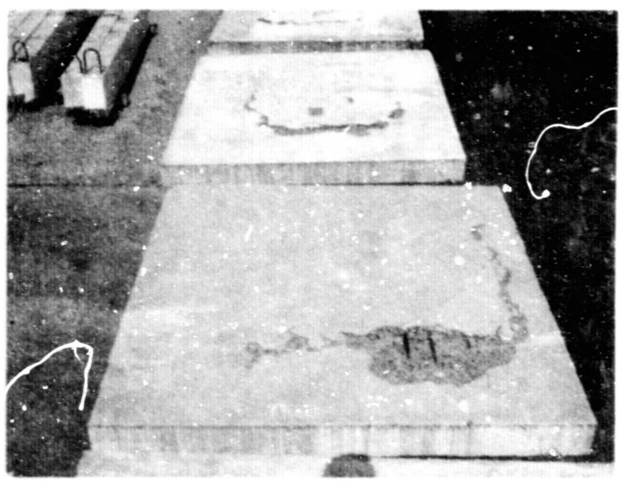

SPECIMEN VII - 7a

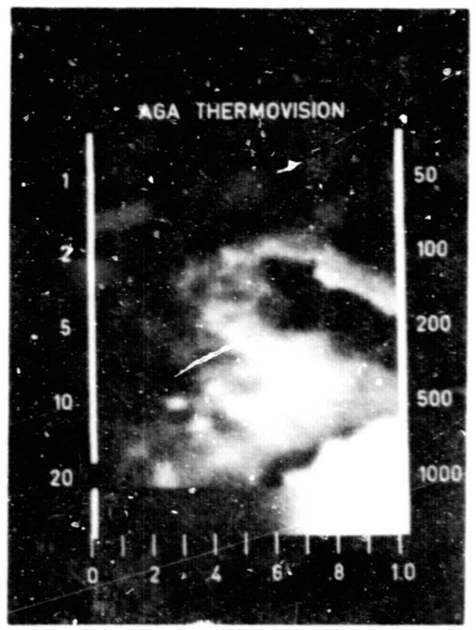

7b 6-6-69 9:55 p.m.
Dark areas delaminated, light areas solid

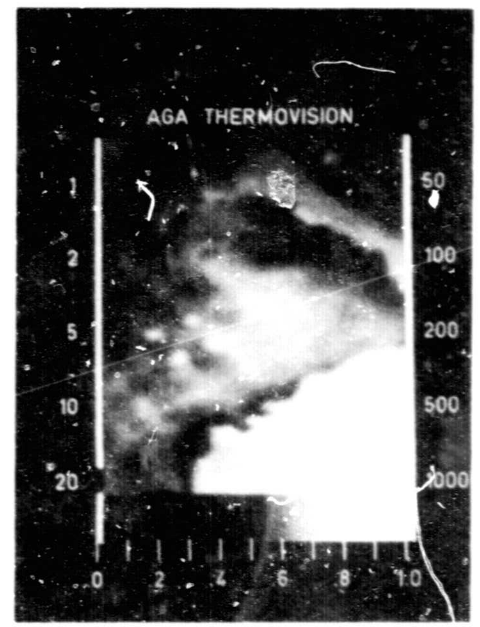

7c 6-6-69 10:00 p.m.
Dark areas delaminated, light areas solid